Biomaterials 32 (2011) 9021–9030

Contents lists available at ScienceDirect

Biomaterials

journal homepage: www.elsevier.com/locate/biomaterials

Assessment of nanomaterial cytotoxicity with SOLiD sequencing-based microRNA expression profiling

Shuchun Li, Haitao Wang, Yuhua Qi, Jing Tu, Yunfei Bai, Tian Tian, Ningping Huang, Yong Wang, Fei Xiong, Zuhong Lu, Zhongdang Xiao*

State Key Laboratory of Bioelectronics, School of Biological Science & Medical Engineering, Southeast University, #2 Si Pai Lou, Nanjing 210096, PR China

ARTICLE INFO

Article history:
Received 2 July 2011
Accepted 10 August 2011
Available online 1 September 2011

Keywords:
MicroRNA
Cytotoxicity
Nanomaterial
SOLiD sequencing

ABSTRACT

The cytotoxicity of nanomaterials has become a major concern in the field of nanotechnology. The key challenge is the lack of reliable methods to examine the overall cellular effects of nanomaterials. Here, a new method is developed to assess the cytological effects of nanomaterial basing on miRNA expression profiling. The SOLiD sequencing is used to acquire the miRNAs expression profiling in NIH/3T3 cells after exposure to Fe_2O_3 NPs, CdTe QDs and MW-CNTs, respectively. The systematic analysis of miRNAs expression profiling is established by taking account of all miRNAs into their regulatory networks. By affecting the output of targeted mRNAs, miRNAs widely regulated the KEGG pathways and GO biological processes in nanomaterial treated cells. Therefore, the miRNA expression profiling can well reflect the characteristic of nanomaterials, and the method not only provide more evidences to assess biocompatibility of nanomaterials and but also clues to discover new biological effects of nanomaterials.

© 2011 Elsevier Ltd. All rights reserved.

1. Introduction

Nanomaterials have received considerable interest recently because of their unique properties and diverse applications in the life science, such as cancer therapy, antimicrobial agents, transfection and medical imaging [1–7]. In contrast with the rapid increase in manufacturing of nanomaterials, the knowledge on cellular effects of nanomaterials is still limited. The cellular effects of nanomaterials become more and more important because of their potential hazards to the humans health and the environment [8–10]. This concern has triggered the emergence of a new scientific discipline of nanotoxicity [11–14]. Unfortunately, few of the studies on nanotoxicity could make a robust conclusion on the cytotoxicity of a certain nanomaterial till now. All difficulties have been originated from the complexity of both nanomaterials and living organisms [15,16], but the crucial challenge is the lack of reliable methods to assess the overall cellular effects of nanomaterials instead of just considering the conventional toxicity assays.

Comparing to the *in vivo* studies, the *in vitro* testing is less ambiguous ethically, easier to control and reproduce and less expensive [17]. The conventional *in vitro* assays include cell culture assays for cytotoxicity (altered metabolism, decreased growth, lytic or apoptotic cell death), proliferation, genotoxicity, and altered gene expression (Northern blot, real-time PCR, microarray, etc.) [18]. For their advantages of high-throughput, the gene expression assays are the important tools for screening the biocompatibility of nanoparticles. For its high-throughput in the measurement of mRNA levels, the detection of mRNA has become the most common method for gene expression assays. But the mRNA degradation in the RNA sample preparation and the regulation in mRNA translation make mRNA assays not truly reflect the gene expression. Therefore, the assay on mRNA levels is not an optimal choice to study the biocompatibility of nanoparticles.

Comparing to the instability of mRNAs, microRNAs (miRNAs) with 21–24 nucleotide length show higher stability in RNA samples [19]. The chromosomal locations of many miRNAs are between genes with their own transcriptional elements, which can make miRNAs regulated and adapted more rapidly adapting to the stimulations [20]. More importantly, some new high-throughput methods, for example the deep sequencing techniques, have been recently set up to successfully detect the miRNA expression profiling [21].

miRNAs have been proved to repress gene expression at the post-transcriptional level and participate in a wide range of cellular processes [22]. The changes in the miRNA expression profiling can globally alter the protein output, which subsequently regulates many key biological processes, including cell growth, death,

* Corresponding author. Tel.: +86 25 83790820.
E-mail address: zdxiao@seu.edu.cn (Z. Xiao).

0142-9612/$ – see front matter © 2011 Elsevier Ltd. All rights reserved.
doi:10.1016/j.biomaterials.2011.08.033

development and differentiation. It is conceivable that miRNAs take part in the cytotoxicity of nanomaterials, which has been confirmed by the involvement of miRNAs in the apoptosis-like cell death [23]. Accordingly, a method is proposed to assess the biocompatibility of nanoparticles *in vitro* by getting miRNAs expression profiling with a newly developed deep sequencing technique (SOLiD sequencing system, ABI).

The diversity and abundance of miRNA targets offer an enormous level of combinatorial possibilities, and suggest that miRNAs and their targets appear to form a complex regulatory network intertwined with other cellular networks. It is reasonable to think that miRNAs exert their functions through regulating cellular networks. Thus, it is imperative to understand how miRNAs take part in cellular processes at a system level. Among those studies on systematic analysis of miRNAs, few studies completely consider the cooperation of miRNAs to their targeted mRNAs [24–28]. And a mathematical model is presented to comprehensively analyze the influences of all miRNAs in nanoparticle treated cells on the gene expression. Then, the significantly regulated genes according to the Z-test were enriched into KEGG pathways with a web-based bioinformatics tool, DAVID.

2. Methods

2.1. Preparation of nanoparticles

High quality oil-soluble CdTe quantum dots were synthesized in liquid paraffin wax according to Xing Bin et al. [29]. Then, the water-soluble CdTe QDs were prepared with short-chain thioglycolic acid (TGA) as described by Wang Yong et al. [30]. Fe_2O_3 NPs and MW-CNTs were offered by our cooperative research group. Transmission electron microscopy (TEM) images were taken with a Tecnai 20 microscope [31]. The TEM samples were prepared by dropping the freshly prepared solution onto a 300-mesh carbon-coated copper grid.

2.2. Cell culture and WST-1 testing

The NIH/3T3 cells (SIBS, China) were cultured in the Dulbecco's Modified Eagle Medium (DMEM) (Gibco, Canada) containing 10% fetal bovine serum (FBS) (Gibco, Canada) and 1% penicillin–streptomycin (Gibco, Canada) at 37 °C in a 5% CO_2 incubator (Hera Cell 150, Thermo).

After exposure to nanomaterials, the viability of NIH/3T3 cells was determined by the WST-1 according to the manufacturer's instruction [32]. For this purpose, cells were seeded in 96-well plates and incubated in DMEM for 24 h followed by stimulation with Fe_2O_3 NPs (50, 100, and 150 μg/ml), MW-CNTs (50, 100, and 150 μg/ml) and CdTe QDs (15, 30, and 45 μg/ml) for 12 h and 24 h, respectively. The assays were performed by adding the WST-1 to the culture wells and incubating them for 2 h at 37 °C. The plates were then read by a scanning multi-well spectrophotometer by measuring the absorbance of the dye with a wavelength of 450 nm. All measurements were taken in triplicate from three or more independent experiments.

After exposure to nanomaterials, the cell survival ratio was calculated with the following formula,

$$\text{Ratio}(\%) = (OD_{\text{test}}/OD_{\text{control}}) \times 100\%. \quad (1)$$

2.3. Small RNA extraction and SOLiD sequencing

The cells were planted at the initial density of 1×10^5 cells ml^{-1} in 35 mm culture dishes. After 24 h of planting, the cells were exposed to 100 μg/ml Fe_2O_3 NPs, 100 μg/ml MW-CNTs and 30 μg/ml CdTe QDs (Fig. 1a) to extract the small RNAs. After exposure to nanomaterials for 24 h, the cells were harvested with the trypsin to extract the small RNAs using the mirVana™ miRNA isolation kit (Ambion) according to the manufacturer's protocol.

Then, the small RNAs in a sample were converted into a double-stranded cDNA library with the SOLiD™ Small RNA Expression Kit (P/N 4397682), which was compatible with the Applied Biosystems SOLiD™ System. The results of SOLiD sequencing were in the form of nucleotide sequences and their coverage. The registered miRNAs were screened out by comparing them in Genbank (www.ncbi.nlm.nih.gov/Genbank) and miRbase (http://www.mirbase.org).

The dysregulated expression of miRNAs in the nanomaterial treated NIH/3T3 cells were analyzed with the fold-change analysis. The coverage of a miRNA in the miRNA group was calculated with the formula (2).

$$\text{Coverage}_{\text{miRNA}} = c_{\text{miRNA}}/C_{\text{miRNA}}, \quad (2)$$

where c_{miRNA} means the count of the miRNA and C_{miRNA} denotes the count of all miRNAs in a small RNA sample. Then, the fold-change of miRNA expression was detected with the following formula (3).

$$\text{Fold}_{\text{miRNA}} = \frac{(\text{Coverage}_{\text{miRNA}})_{\text{test}} \times 10^6}{(\text{Coverage}_{\text{miRNA}})_{\text{control}} \times 10^6} = \frac{(c_{\text{miRNA}}/C_{\text{miRNA}})_{\text{test}} \times 10^6}{(c_{\text{miRNA}}/C_{\text{miRNA}})_{\text{control}} \times 10^6}. \quad (3)$$

2.4. qRT-PCR

To confirm the differential expression of miRNAs in the NIH/3T3 cells after Fe_2O_3 NP and CdTe QD treatment, we performed some miRNAs tests with stem-loop Q-PCR assays in small RNA samples isolated from nanoparticle treated NIH/3T3 cells and the control, respectively.

miRNAs were reverse-transcribed with the loop primers (Supplement Table 1). The cDNA synthesis was performed with a 2720 Thermal Cycler (Applied Biosystems) in a 20 μl reaction volume containing 1 μg total RNA, 0.5 μM reverse-transcript primers, 50 mM Tris–HCl (pH 8.3), 75 mM KCl, 3 mM $MgCl_2$, 10 mM dithiothreitol, 20 units ribonuclease inhibitor and 100 U PrimerScript™ reverse transcriptase (Takara, China). After incubation at 42 °C for 1 h, the reverse transcriptase was inactivated at 85 °C for 5 min and the cDNAs were stored at −20 °C or immediately used for real-time PCR.

After the cDNA synthesis, the relative expression levels were determined by real-time PCR in an ABI 7500 real-time PCR system with Evagreen (Biotium, USA). All reactions were performed in triplicate with the same cDNA samples and, hence, represented technical replicates. The Takara Tag™ Hot Start version (Takara, China) was used according to the manufacturer's suggestions. Briefly, 1 μl cDNA was used for a 20 μl PCR reaction containing 0.5 U Tag™ Hot Start PCR enzyme, 0.2 mM dNTPs, 0.4 μM forward primer, 0.4 μM reward primer, 1 μl Evagreen, 0.4 μl ROX (Takara, China). PCR was achieved with a 10 min activation and denaturation step at 95 °C, followed by 40 cycles of 15 s at 95 °C and 60 s at 60 °C. The baselines and the thresholds for Ct calculation were set automatically with the ABI Prism 7500 SDS software version 1.1, or set manually whenever necessary.

The expression levels of candidate miRNAs were measured in terms of threshold cycle value (Ct) and normalized to the small nuclear RNA U6. The ratio of miRNAs in two groups was calculated by using the equation $2^{-\Delta\Delta Ct}$, and the $-\Delta\Delta$Ct were calculated with the following formula,

$$-\Delta\Delta Ct = -\left[(Ct_{\text{miRNA}} - Ct_{U6})_{\text{test}} - (Ct_{\text{miRNA}} - Ct_{U6})_{\text{control}}\right]. \quad (4)$$

2.5. Repression to mRNAs by miRNAs

The degree of miRNA repression to a specific $mRNA_k$ was calculated with the following formula.

$$R_{mRNA_k} = \left[\sum_{i=1}^{n}(\text{Count}_{miRNA_i}/n_{ij})\right] \Big/ N_{\text{total}}, \quad (5)$$

in which, $R_{mRNA\ k}$, the repression degree to the $mRNA_k$ by its targeted miRNAs; Count_{miRNAi}, the count of the *ith* miRNA; i, the number of miRNAs target to the $mRNA_k$, $i = 1, 2, \ldots, n$; n_{ij}, the number of mRNAs targeted by the $miRNA_i$; N_{total}, the number of all miRNAs detected in a small RNA sample.

2.6. Bioinformatics analysis

The database alignment of sequences obtained from the SOLiD sequencing was performed with the Genbank and miRbase databases, to screen out the mature miRNAs in a small RNA sample. Following the acquisition of expression patterns of miRNAs, the fold-change analysis was performed to get differentially expressed miRNAs.

Subsequently, the KEGG pathways and the GO biological processes significantly affected in nanoparticle treated NIH/3T3 cells were detected with the procedures in Fig. 2. Briefly, the repression of mRNAs by miRNAs was calculated with the formula proposed in this paper. Then, the genes significantly affected after nanoparticle exposure were obtained with the Z-test. Finally, the genes significantly affected were enriched to either the KEGG pathways or the GO biological processes through DAVID bioinformatics.

2.7. Statistical analysis

The *Z*-test assay was performed to investigate the differences in the repression of target mRNAs by miRNAs in nanomaterial treated NIH/3T3 cells. p_0 was calculated by the formula (6), which was the estimate of the proportions if the null hypothesis was true.

$$p_{0k} = \frac{[R_{mRNAk} \cdot N_{\text{total}}]_{\text{test}} + [R_{mRNAk} \cdot N_{\text{total}}]_{\text{control}}}{N_{\text{total test}} + N_{\text{total control}}}. \quad (6)$$

$$Z_k = \frac{R_{mRNAk\ \text{test}} - R_{mRNAk\ \text{control}}}{\sqrt{p_{0k}(1-p_{0k})/N_{\text{total test}} + p_{0k}(1-p_{0k})/N_{\text{total control}}}}. \quad (7)$$

When the Z-value >1.96 or <1.96, the null hypothesis was rejected, which meant that there were significant differences between the repression of mRNAs in the nanomaterial treated cells and the control cells.

3. Results and discussions

3.1. Cytotoxicity of nanomaterials in NIH/3T3 cells

Among the methods applied to investigate the cytotoxicity of nanomaterials, the tetrazolium based methods (such as MTT, WST-1, and WST-8 etc.) are commonly used to test the cytotoxicity. After exposure to nanomaterials for 12 h and 24 h, the cellular survival ratio was measured with WST-1. The results indicated that the cytotoxicity of nanomaterials had time- and dose-dependent tendencies (Fig. 1b and Supplementary Fig. 1), which were consistent with previous reports [33,34]. After exposure to CdTe QDs with the lowest concentration (15 μg/ml), the cellular survival ratio was lower than those after exposure to Fe_2O_3 NPs and MW-CNTs with the highest concentration (150 μg/ml), which indicated that CdTe QDs had more cytotoxicity than Fe_2O_3 NPs and MW-CNTs. Fe_2O_3 NPs show more cytotoxicity than MW-CNTs at the same concentration. Thus, a certain exposure concentration (100 μg/ml for Fe_2O_3 NPs, 100 μg/ml for MW-CNTs and 30 μg/ml for CdTe QDs) for nanomaterial to NIH/3T3 cells were chosen for the subsequent analysis.

Another simple cytotoxicity test involved the visual inspection of the cells with a bright-field microscopy for the changes in cellular morphology. After exposure to nanomaterials applied in this paper with the concentrations as described above, the cellular morphology were widely affected, especially those exposed to Fe_2O_3 NPs and CdTe QDs (Fig. 1c and Supplementary Figs. 2–4), which was in accordance with the results of WST-1 assay.

3.2. Expression profiling of miRNAs with SOLiD sequencing

To explore the involvement of miRNAs in the cytotoxicity of nanomaterials, the expression patterns of miRNAs were analyzed with a high-throughput deep sequencing method (SOLiD sequencing) after exposure to nanomaterial. A total of tens millions SOLiD sequencing reads were obtained from the small RNA samples extracted from the each nanomaterial treated cells and the control cells. The size distribution of sequencing reads showed that the majority of sequences were 18–25 nt long (about 90%), with 22 nt length being the most abundant (Fig. 3a), which was within the typical size range of miRNAs. After filtrating the reads contaminated by other RNA pieces and comparing with miRBase database, we got several hundred kinds of miRNA with total copies of several hundreds of thousands for each sample (162, 172 and 149 miRNAs in Fe_2O_3 NP, MW-CNT and CdTe QD treated cells, respectively).

The coverage of many miRNAs (about 70%) was lower than 0.001, which suggested the feasibility of SOLiD sequencing in detecting miRNAs with low coverage (Fig. 3a and Supplementary Fig. 5). We then analyzed the correlation between the coverage of miRNAs in the each nanomaterial treated cells and the control cells. Although some miRNAs with the correlation largely deviated from

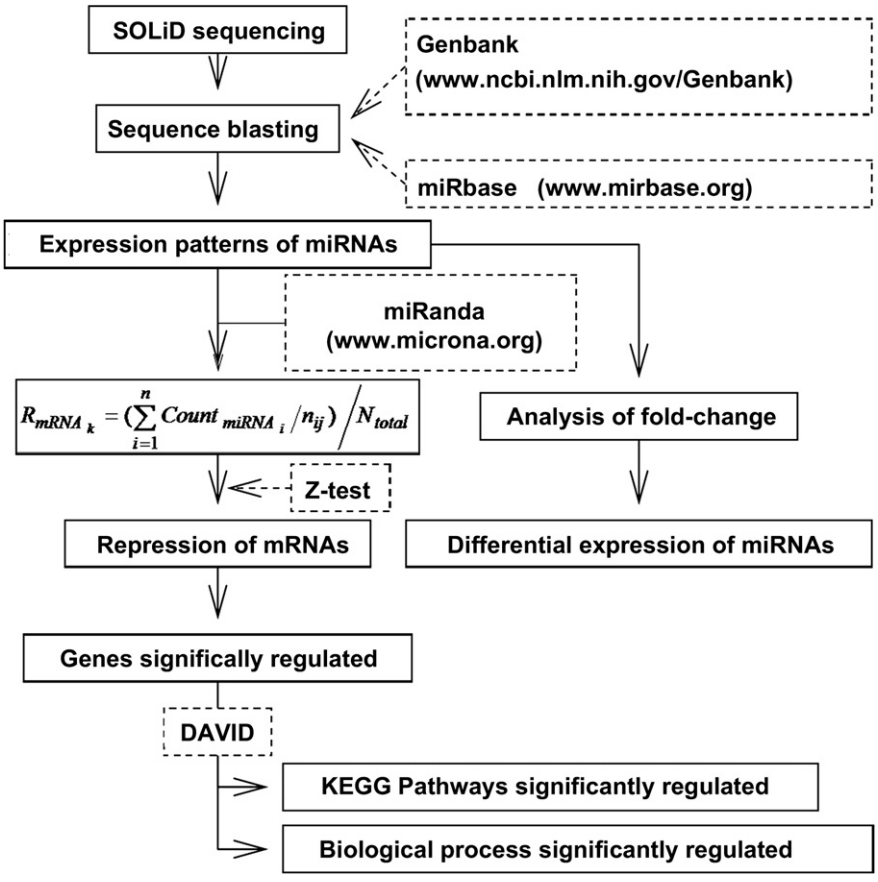

Fig. 1. Flow diagram of assessing nanomaterial cytotoxicity.

one in nanomaterial treated cells, most miRNAs were slightly regulated (Fig. 3b), which was confirmed by the subsequent fold-change analysis. According to the fold-change analysis, the expression levels of miRNAs were widely affected (Fig. 3c). Comparing to the expression levels of miRNAs in cells treated by Fe_2O_3 NP and CdTe QD, the expression levels of miRNAs in MW-CNT treated cells were more tempestuously regulated. Thus, the dysregulated expression of miRNAs could be induced by nanomaterial exposure.

To verify the accuracy of SOLiD sequencing method for measuring the expression patterns of miRNAs, we analyzed the same RNA samples by detecting some miRNAs with the qRT-PCR, which was generally accepted as an accurate method for measuring relative expression levels of miRNAs. In Fe_2O_3 NP and CdTe QD treated cells, the expression levels of some miRNA were measured with the qRT-PCR (Fig. 3d). The correlation between the expression levels of miRNAs obtained with the SOLiD sequencing and the qRT-PCR was clear and statistic significant (Fig. 3e). Therefore, the expression patterns of miRNA detected by the SOLiD sequencing could be acceptable for judging the relative expression of miRNAs.

Another valuable feature of miRNA expression profiling was that there were some co-regulated miRNAs in different nanomaterial treated cells. Except for those miRNAs co-regulated in all the three nanomaterial treated cells (such as miR-34s, miR-21 and miR-29a etc.), many miRNAs were co-regulated after two out of three nanomaterial exposure (Fig. 3f and Supplementary Table 2), which suggested the similarity of cytotoxicity of nanomaterials.

Although the dysregulated expression of miRNAs can start from the transcription of pri-miRNAs and be strengthened at the processing of miRNA maturation [23], the transcription of pri-miRNAs is the most important step for its complex regulation. The mechanisms of the epigenetic control and the Pol II-associated transcription factors have been reported to take part in the regulation of pri-miRNA transcription [35,36], which can be affected after nanoparticle exposure [37]. Choi et al. finds that the CdTe QD treatment can induce global hypoacetylation implying a global epigenomic response, and activate *p53* by phosphorylation at the post-translational level [37]. The expression levels of many miRNAs can be activated by the phosphorylated *p53*, including miR-34 family miRNAs (miR-34a, miR-34b and miR-34c). The co-regulated expression of miR-34s suggested the activation of *p53* in nanomaterial treated NIH/3T3 cells. Thus, the transcription of pri-miRNAs allows miRNA genes to be elaborately regulated in specific conditions.

3.3. Mathematical model for repression to mRNAs by miRNAs

In the previous analysis of miRNA expression profiling obtained by deep sequencing, only miRNAs with significant differences has

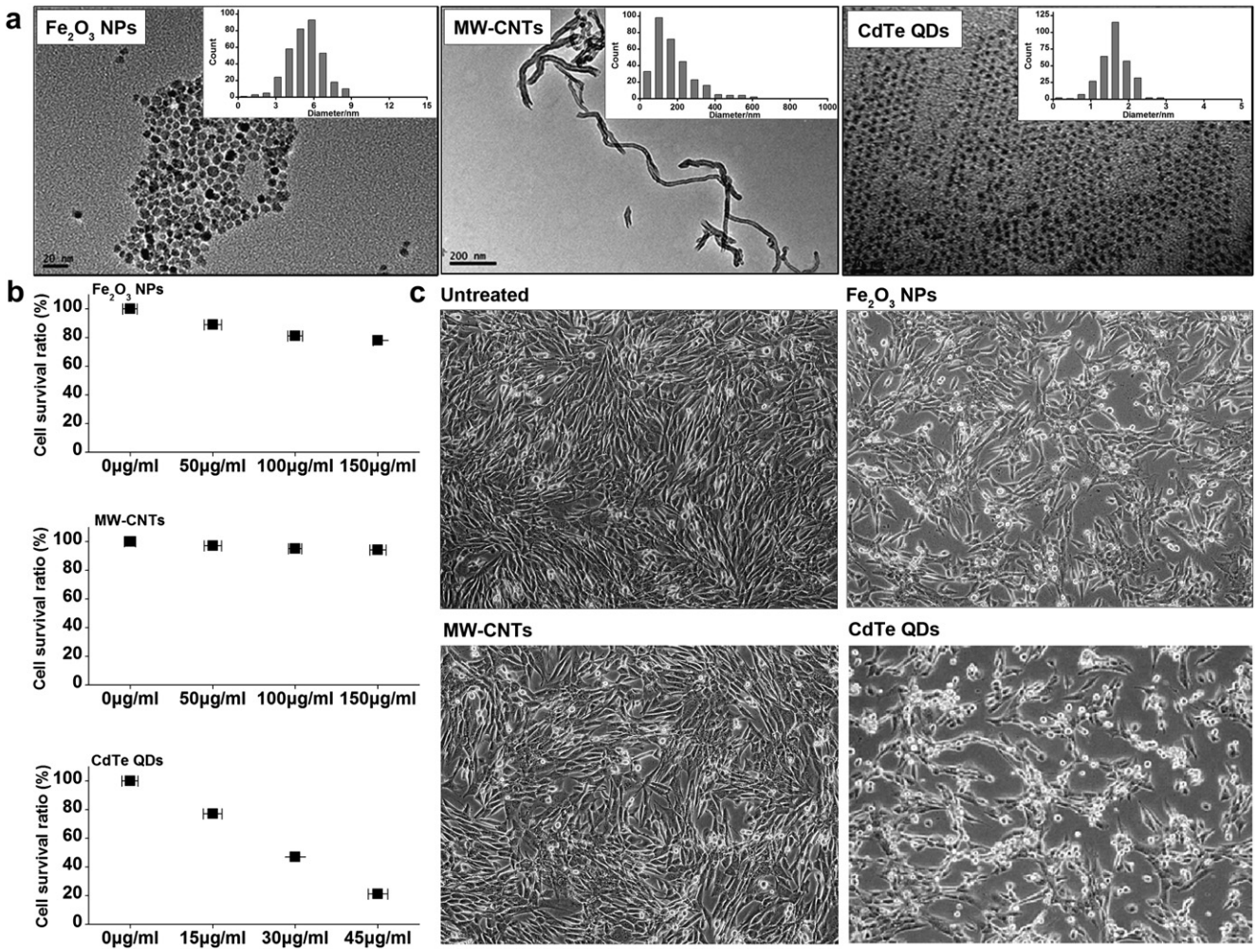

Fig. 2. Cytotoxicity of nanomaterials. After the exposure to 100 μg/ml Fe_2O_3 NPs, 100 μg/ml MW-CNTs, and 30 μg/ml CdTe QDs (a) for 24 h, the cell survival ratio were decreased (b), and the cellular morphology were also affected (c).

been concerned while those miRNAs with high coverage and less significant difference are neglected [26], which results in the incomplete understanding of miRNA expression profiling. Consequently, we developed a new analysis method to make a more reliable annotation for the miRNAs data by concerning all miRNAs. In this new method, all miRNAs detected by the deep sequencing were firstly assigned to all their targeted mRNAs according to a principle that each miRNA has equal possibility to bind its target

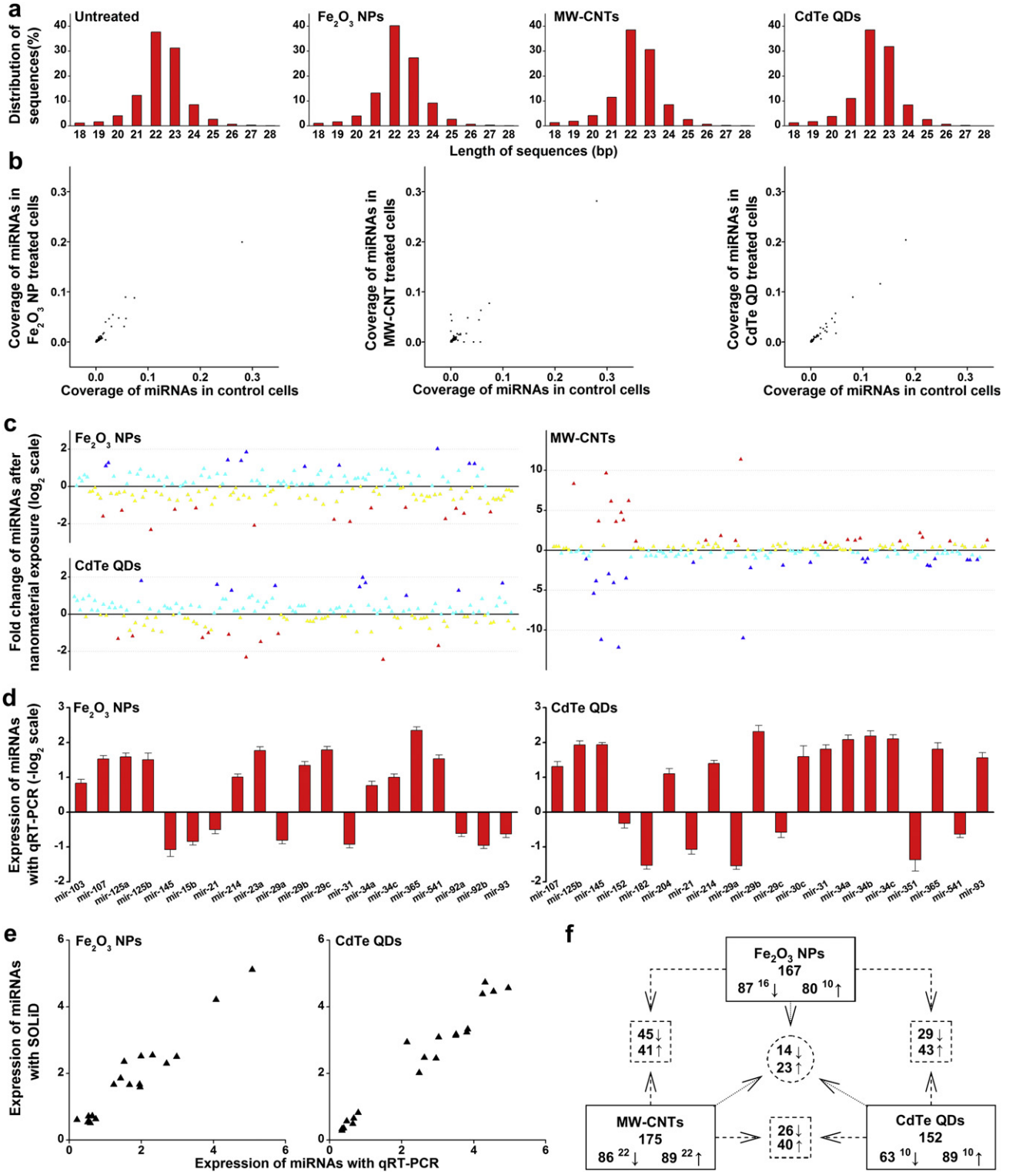

Fig. 3. miRNA results of SOLiD sequencing. (a) The length distribution for small RNAs detected by the SOLiD sequencing. These sequences with 21–24 nucleotides length covered the most number in all detected sequences. miRNAs were identified by blasting miRNA database. (b) The correlations of miRNA coverage between the nanomaterials-treated samples and the untreated group. (c) The differential expression of miRNAs with the fold-change analysis in SOLiD sequencing. (d) The differential expression of miRNAs detected by the quantitative real-time PCR. (e) The significant relationship between the differential miRNA expression detected by the SOLiD sequencing and the qRT-PCR. (f) The number of miRNAs co-affected by different nanomaterials.

mRNAs respectively, and the total coverage to a certain mRNA were then summed up from all kinds of miRNAs.

The mechanism of mRNA down-regulation is modeled by considering the concentrations of mRNA in three different forms, the free mRNA, the mRNA bound in the mRNA–miRNA complex, and the mRNA localized to P-bodies [38]. And the translation of a mRNA is obviously determined by the concentrations of its free mRNA [39]. In other words, the repression of translation of the mRNA is caused by binding of the miRNAs to their target in both of the latter cases [40]. Thus, the degree of miRNA repression to its targeted mRNAs can be determined by the coverage of mRNA–miRNA complexes. With the in-depth study of miRNA mechanisms, the mathematic model could be modified to synthetically investigate the functions of miRNAs at the system level.

In the maturation of miRNAs, the rate of miRNA formation from the dsRNA is lower than that of miRNA-loaded RISC formation [41,42], which means that the formation of the miRNA-loaded RISC occurs simultaneously with the miRNA formation. The competitive interaction between the targeted mRNAs of a certain miRNA suggests that the miRNA-loaded RISC can be arrested by mRNAs to decoy their suppression mechanisms [43]. Thus, the miRNAs detected in the SOLiD sequencing are those loaded into the RISC combining targeted mRNAs.

3.4. Adaptive translation of mRNAs by miRNAs after nanomaterial exposure

According to the formula provided above, the repression degrees of miRNAs to their target mRNAs in nanomaterial treated cells were obtained (Fig. 4a). About 5387, 5336 and 5410 mRNAs were repressed by miRNAs in Fe_2O_3 NP, MW-CNT and CdTe QD treated cells, respectively. Subsequently, the Z-test was performed to compare the differences between the repression of miRNAs in control cells and nanomaterial treated cells. The Z-test results indicated that many mRNAs were significantly repressed by miRNAs after nanomaterial exposure (Fig. 4a). But those mRNAs significantly repressed by miRNAs occupied a small proportion of all targeted mRNAs, about 16.13%, 9.05% and 17.75% in Fe_2O_3 NP, MW-CNT and CdTe QD treated cells, respectively.

As mentioned above, the translation of mRNAs base on the concentration of free mRNAs, which can be affected by the competitive presence of mRNA–miRNA complexes. The mRNAs, which are more combined by miRNAs to form mRNA–miRNA complexes, will be less translated to proteins. Thus, we got a list of mRNAs whose translation would be significantly affected. The genes significantly up-regulated were more than those significantly down-regulated after nanomaterial exposure (Fig. 4b), which was due to the dysregulated expression of miRNAs. When the mount of RISC was decreased for the down-regulation of miRNAs, the repression to their targeted mRNAs would be weakened.

A relatively small group of 869 genes (approximately 16% of total regulated genes), 453 up-regulated and 416 down-regulated, were significantly affected by Fe_2O_3 NPs and 960 genes, 594 up-regulated and 366 down-regulated by CdTe QDs while the amount of significantly affected genes was approximately half of them in MW-CNT treated samples (483 genes of which 266 up-regulated and 217 down-regulated) (Fig. 4b). These results might be consistent with the phenomenon that MW-CNT induced less cells morphologically changing than that of Fe_2O_3 NPs and CdTe QDs (Fig. 1c). To explore the co-affected genes among nanomaterials can help to understand the cytotoxicity of nanomaterials (Fig. 4c). Approximately 20% of genes significantly regulated were consistently affected by both Fe_2O_3 NPs and CdTe QDs (181 genes of which 88 up-regulated and 93 down-regulated). There were 65 consistently affected genes of which 59 were up-regulated while 6 were down-regulated between CdTe QDs and MW-CNT and only 20 down-regulated co-affected genes between Fe_2O_3 NPs and MW-CNT. These consistently affected genes can help to understand the common cytological effect of different nanomaterials.

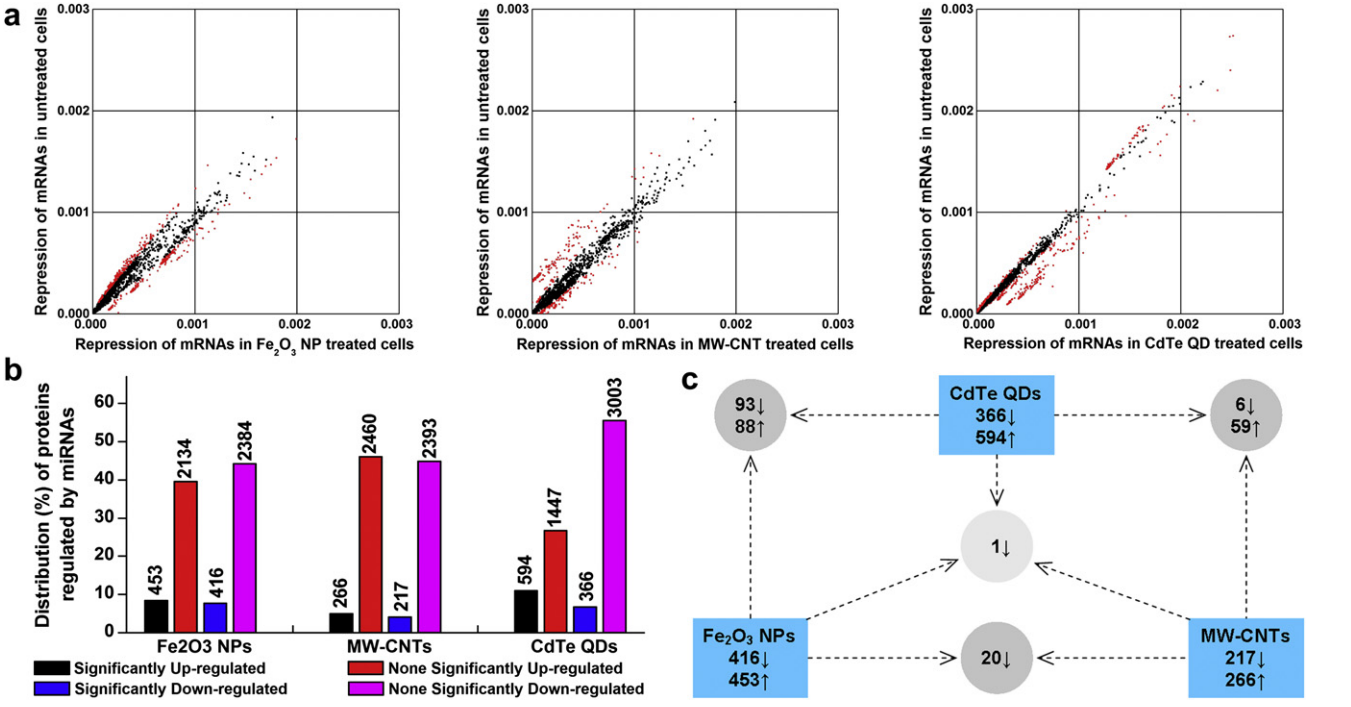

Fig. 4. Changes of gene expression at translation level regulated by miRNAs. (a) The correlation between the repression of mRNAs by miRNAs in nanomaterial treated cells and untreated cells. (b) The distribution of regulated genes. The number marked upon each column means the amount of genes involved in different categories. (c) The comparison of significantly affected genes among the three nanomaterials.

3.5. Differential regulation of KEGG pathways in nanomaterial cytotoxicity

The KEGG pathway database records networks of molecular interactions in the cells [44]. We then applied the DAVID to enrich those genes significantly affected by nanomaterial exposure into KEGG pathways. By doing that, we found that many KEGG pathways were significantly affected after nanomaterial exposure (Fig. 5a). Although all pathways significantly affected could be rooted to main branches in KEGG Pathway database, many pathways were rooted as signal transduction pathways to process environmental information (Fig. 5a), which suggested that the stimulation of nanomaterials could be declined or amplified by those signal transduction pathways. Thus, dysregulated expression of miRNAs was an adaptive process to external stimuli.

Among those significantly regulated KEGG pathways, the WNT signaling pathway and the MAPK signaling pathway were co-affected after exposure to all the three nanomaterials chosen in this paper, which suggested the presence of common mechanism. 93 and 88 genes were down- and up-regulated after Fe_2O_3 NP and CdTe QD exposure, respectively (Fig. 4c). Even though significant differences between the cytotoxicity of Fe_2O_3 NPs and CdTe QDs had been found (Fig. 2), significantly co-affected KEGG pathways were still present in NIH/3T3 cells treated by the two nanoparticles. Two KEGG pathways rooted to cell communication (gap junction and adherens junction) and another two pathways rooted to signal transduction (TGF-beta signaling pathway and Notch signaling pathway) were co-affected in Fe_2O_3 NP and CdTe QD treated cells, which then broken off the junction and blocked the information exchange between cells. And the changes in cell morphology with a bright-field microscopy confirmed the destruction of cell junction.

Among those significantly affected KEGG pathways after nanoparticle exposure, some KEGG pathways were only affected by one of the three nanomaterials (Fig. 5a). For the good biocompatibility of MW-CNTs (Fig. 2b), only three KEGG pathways were significantly regulated by microRNAs in MW-CNT treated cells. Except for the two pathways co-affected by all the three nanomaterials, the regulation of actin cytoskeleton was the only pathway which was significantly regulated in MWCNT treated cells (Fig. 5a), which then affected the normal structure of actin cytoskeleton. These results were similar to the results of the previous report [45].

Anionic dimercaptosuccinic acid (DMSA)-coated iron oxide nanoparticles are readily endocytosed by cells and are found either in the cytoplasm, inside endosomes, or accumulated in the perinuclear region within the cells [46–48]. Changes in cell morphology were observed after nanoparticle exposure with the cells assuming a spherical shape with disruption of the cell cytoskeleton [48]. And Fe_2O_3 nanoparticles diminish cellular proliferation and affect the actin cytoskeleton as well as focal adhesion formation and maturation [48]. We found that two KEGG pathways, focal adhesion and regulation of actin cytoskeleton, were significantly affected in Fe_2O_3 NP treated NIH/3T3 cells, which could partly explain the changes in cell morphology.

The cytotoxicity of CdTe QDs has been discussed in several reports. And the mechanisms of CdTe QDs toxicity are focused on the release of Cd^{2+} and the generation of ROS in the state of oxidative stress. Consequently, generated ROS and released Cd^{2+} jointly trigger a series of radical chain reactions, cause lipid peroxidation, and lead to cell apoptosis. Among those reactions, the activation of *p53* by post-translational mechanisms is a key step in the induction of cell apoptosis after CdTe QD exposure [23,37]. The DAVID results indicated that the *p53* pathway was significantly affected by CdTe QD exposure (Fig. 6). Among the eight significantly regulated genes involved in the pathway, four genes including PUMA, Gadd45, Siah and Siah-1 were up-regulated, and the others were down-regulated. The down-regulated expression of Cyclin E can repress the transition from G_1 to S phase.

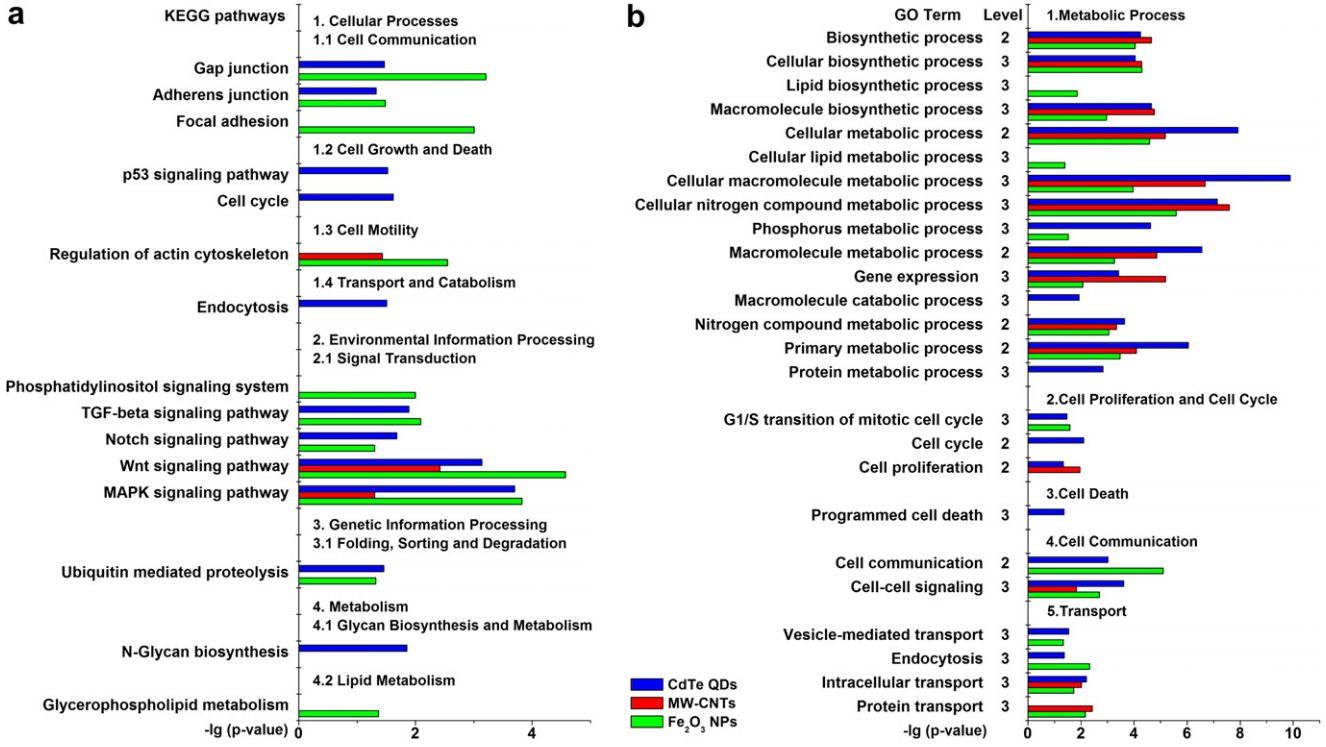

Fig. 5. Assessment of Nanomaterial Cytotoxicity. The KEGG pathways (a) and GO terms (b) significantly by miRNAs in nanomaterial treated NIH/3T3 cells.

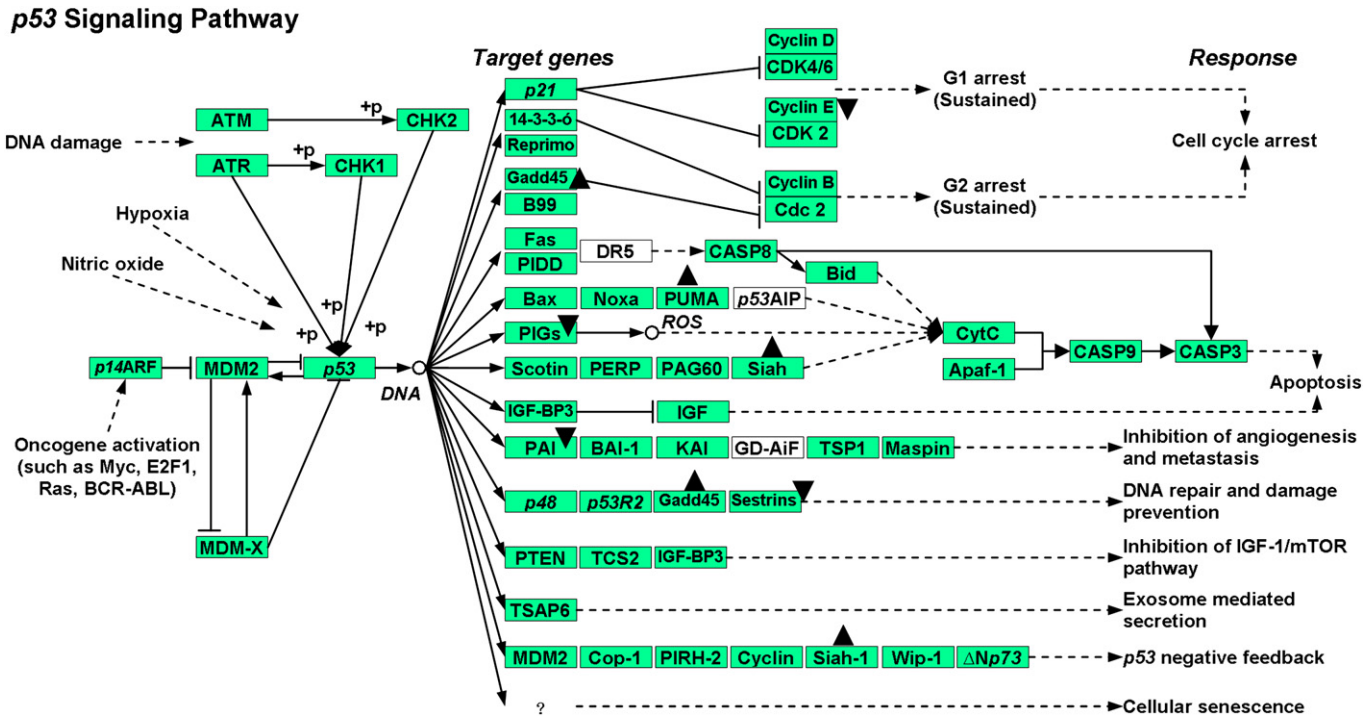

Fig. 6. *p53* signaling pathway significant affected in CdTe QD treated cells. ▲, the genes with up-regulated expression; ▼, the genes with down-regulated expression.

3.6. Effects of nanomaterials on GO biological processes

The Gene Ontology (GO) provides the ontology of defined terms representing gene product properties [49]. Among the three covered domains by the GO, the Biological Process, operations or sets of molecular events with a defined beginning and end, can relevantly describe the functioning of integrated genes. Based on the significantly regulated genes, the biological processes involved in the cytotoxicity of nanomaterials were assessed with the web-based GO analysis tool, DAVID. By doing that, we assessed the cytotoxicity of nanomaterials at the system level.

Among those significantly affected GO terms, most of them were rooted to the regulation of processes for each nanomaterial (Supplementary Tables 3–5), which suggested that cells intended to adjust themselves to the environmental change after exposure to nanomaterials. Except for those GO terms rooted to regulation, the significantly regulated GO terms were roughly divided into five categories (metabolic process, cell proliferation and cell cycle, cell death, cell communication, and transport) to comprehensively analyze the cytotoxicity of nanomaterials (Fig. 5b).

After exposure to nanomaterials, the reduction in cell viability had measured with the WST-1 analysis (Fig. 2b) in this paper, which suggested that intracellular metabolic processes should be affected. The results of DAVID analysis indicated that some GO terms rooted to the metabolic process were widely regulated in nanomaterial treated NIH/3T3 cells (Fig. 5b). Among those GO terms, many terms were co-regulated after exposure to all the three nanomaterials. For example, five GO term at the level two (biosynthesis process, cellular metabolic process, macromolecular metabolic process, nitrogen compound metabolic process, and primary metabolic process) were significantly regulated in nanomaterial treated NIH/3T3 cells, which reflected the common cytological effects induced by nanomaterial exposure.

For MW-CNTs with the lowest cytotoxicity, some metabolic processes were solely regulated either by Fe_2O_3 NPs or CdTe QDs. After exposure to 100 μg/ml Fe_2O_3 NPs for 24 h, the lipid biosynthetic process and the cellular lipid metabolic process were significantly affected. Combining the glycerol-phospholipid metabolism KEGG pathway, the lipid metabolism was found in Fe_2O_3 NP treated cells, which had not been analyzed in previous papers. But the macromolecular catabolic process and the protein metabolic process were significantly regulated after exposure to 30 μg/ml CdTe QDs for 24 h, and then affected protein metabolism and modification.

According to the observed results with a phase contrast microscope, the disruption of cell–cell junction and the changes in the cell morphology were induced in nanomaterial treated cells (Fig. 2c), which suggested the possibility of involving the regulation of cell communication and cell proliferation in nanomaterial treated cells. Except for the cell–cell signaling GO term was co-regulated by nanomaterials, the cell communication was affected in Fe_2O_3 NP and CdTe QD treated cells, and it was consistent with the results of KEGG pathways.

The regulation of cellular processes is widely triggered after nanomaterial exposure, including the dysregulated expression of microRNAs. Among those cellular processes, the transport (containing the internalization of nanomaterials and the directed movement of substances within a cell) played an important role in the self-adaption to nanomaterial exposure. We found that the intracellular transport GO term were co-affected by nanomaterials, and it could slow the spread of the damaged substances. The exposure to Fe_2O_3 NPs and CdTe QDs could obviously induce cytotoxicity, and the cytotoxicity of nanomaterials was dependent on the quantity of internalized nanomaterials. The endocytosis, which was a major pathway for the internalization of Fe_2O_3 NPs (Supplementary Fig. 6) and CdTe QDs (Supplementary Fig. 7), was actively regulated to reduce the intake of nanomaterials (Fig. 5b). In addition the vesicle-mediated transport was also regulated in Fe_2O_3 NP and CdTe QD treated cells.

The apoptosis-like cell death is induced by CdTe QD exposure indicated that the expression levels of apoptosis-related proteins should be modulated. According to the results of KEGG pathways,

some apoptosis-related proteins were significantly regulated in CdTe QD treated cells (Fig. 6). As a result, the programmed cell death GO term was found to be affected after exposure to CdTe QDs (Fig. 5b), which was in line with earlier reports that CdTe QD could induce cell death to a variety of cell types [37,50] and our further investigation [23]. In addition, the regulation of cell cycle and the G_1/S transition of mitotic cell cycle were also significantly regulated in this apoptosis process, and provided a basis for analyzing the cytotoxicity of CdTe QDs at the system level.

4. Conclusions

The high-throughput sequencing method was a powerful tool in analyzing the miRNA expression profiling. In this study, the miRNA expression profiling were obtained with the SOLiD sequencing in nanomaterial (Fe_2O_3 NPs, MW-CNTs and CdTe QDs) treated NIH/3T3 cells. After nanomaterial exposure, the expression of miRNAs were widely dysregulated, which highlighted the involvement of miRNAs in the nanomaterial cytotoxicity as regulators at the post-transcriptional level. After exposure to nanomaterials chosen in this paper, the translation of target mRNAs was systematically regulated by all miRNAs in NIH/3T3 cells, which provided a strategy to comprehensively investigate the miRNAs' function. Among all target mRNAs of miRNAs, those mRNAs with significantly regulated translation were enriched into the KEGG pathways and the GO biological processes, respectively. In nanomaterial treated NIH/3T3 cells, many KEGG pathways and GO biological processes were significantly regulated, which provided more evidences to assess the nanomaterial cytotoxicity. By doing that, a new method based on miRNAs expression profiling was developed to assess the nanomaterial cytotoxicity at the system level.

Acknowledgment

This work was financially supported by the National Basic Research Program of China (973 Program: 2007CB936300), NSFC (No. 61071047, No. 30870626) and 2008DFA51180.

Appendix. Supplementary material

The supplementary data associated with this article can be found in the on-line version at doi:10.1016/j.biomaterials.2011.08.033.

References

[1] Kim JW, Galanzha EI, Shashkov EV, Moon HM, Zharov VP. Golden carbon nanotubes as multimodal photoacoustic and photothermal high-contrast molecular agents. Nat Nanotechnol 2009;4:688–94.
[2] Galanzha EI, Shashkov EV, Kelly T, Kim JW, Yang L, Zharov VP. In vivo magnetic enrichment and multiplex photoacoustic detection of circulating tumour cells. Nat Nanotechnol 2009;4:855–60.
[3] Bharali DJ, Khalil M, Gurbuz M, Simone TM, Mousa SA. Nanoparticles and cancer therapy: a concise review with emphasis on dendrimers. Int J Nanomedicine 2009;4:1–7.
[4] Kim JS, Kuk E, Yu KN, Kim JH, Park SJ, Lee HJ, et al. Antimicrobial effects of silver nanoparticles. Nanomedicine 2007;3:95–101.
[5] Mao HQ, Roy K, Troung-Le VL, Janes KA, Lin KY, Wang Y, et al. Chitosan-DNA nanoparticles as gene carriers: synthesis, characterization and transfection efficiency. J Control Release 2001;70:399–421.
[6] Medintz IL, Uyeda HT, Goldman ER, Mattoussi H. Quantum dot bioconjugates for imaging, labelling and sensing. Nat Mater 2005;4:435–46.
[7] Farokhzad OC, Langer R. Impact of nanotechnology on drug delivery. ACS Nano 2009;3:16–20.
[8] Bai Y, Zhang Y, Zhang J, Mu Q, Zhang W, Butch ER, et al. Repeated administrations of carbon nanotubes in male mice cause reversible testis damage without affecting fertility. Nat Nanotechnol 2010;5:683–9.
[9] Barnard AS. One-to-one comparison of sunscreen efficacy, aesthetics and potential nanotoxicity. Nat Nanotechnol 2010;5:271–4.
[10] Thomas CR, George S, Horst AM, Ji Z, Miller RJ, Peralta-Videa JR, et al. Nanomaterials in the environment: from materials to high-throughput screening to organisms. ACS Nano 2011;5:13–20.
[11] Oberdörster G, Oberdörster E, Oberdörster J. Nanotoxicology: an emerging discipline evolving from studies of ultrafine particles. Environ Health Perspect 2005;113:823–39.
[12] Scheringer M. Nanoecotoxicology: environmental risks of nanomaterials. Nat Nanotechnol 2008;3:322–3.
[13] AshaRani PV, Low Kah Mun G, Hande MP, Valiyaveettil S. Cytotoxicity and genotoxicity of silver nanoparticles in human cells. ACS Nano 2009;3:279–90.
[14] Nel A, Xia T, Madler L, Li N. Toxic potential of materials at the nanolevel. Science 2006;311:622–7.
[15] Jiang W, Kim BY, Rutka JT, Chan WC. Nanoparticle-mediated cellular response is size-dependent. Nat Nanotechnol 2008;3:145–50.
[16] Nel AE, Madler L, Velegol D, Xia T, Hoek EM, Somasundaran P, et al. Understanding biophysicochemical interactions at the nano-bio interface. Nat Mater 2009;8:543–57.
[17] Lewinski N, Colvin V, Drezek R. Cytotoxicity of nanoparticles. Small 2008;4:26–49.
[18] Hillegass JM, Shukla A, Lathrop SA, MacPherson MB, Fukagawa NK, Mossman BT. Assessing nanotoxicity in cells in vitro. Wiley Interdiscip Rev Nanomed Nanobiotechnol 2010;2:219–31.
[19] Mraz M, Malinova K, Mayer J, Pospisilova S. MicroRNA isolation and stability in stored RNA samples. Biochem Biophys Res Commun 2009;390:1–4.
[20] Bartel DP. MicroRNAs: genomics, biogenesis, mechanism, and function. Cell 2004;116:281–97.
[21] Git A, Dvinge H, Salmon-Divon M, Osborne M, Kutter C, Hadfield J, et al. Systematic comparison of microarray profiling, real-time PCR, and next-generation sequencing technologies for measuring differential microRNA expression. RNA 2010;16:991–1006.
[22] He L, Hannon GJ. MicroRNAs: small RNAs with a big role in gene regulation. Nat Rev Genet 2004;5:522–31.
[23] Li S, Wang Y, Wang H, Bai Y, Liang G, Huang N, et al. MicroRNAs as participants in cytotoxicity of CdTe quantum dots in NIH/3T3 cells. Biomaterials 2011;32:3807–14.
[24] Gusev Y. Computational methods for analysis of cellular functions and pathways collectively targeted by differentially expressed microRNA. Methods 2008;44:61–72.
[25] Papadopoulos GL, Alexiou P, Maragkakis M, Reczko M, Hatzigeorgiou AG. DIANA-mirPath: integrating human and mouse microRNAs in pathways. Bioinformatics 2009;25:1991–3.
[26] Tan KS, Armugam A, Sepramaniam S, Lim KY, Setyowati KD, Wang CW, et al. Expression profile of MicroRNAs in young stroke patients. PLoS One 2009;4:e7689.
[27] Lafferty-Whyte K, Cairney CJ, Jamieson NB, Oien KA, Keith WN. Pathway analysis of senescence-associated miRNA targets reveals common processes to different senescence induction mechanisms. Biochim Biophys Acta 2009;1792:341–52.
[28] Chen GQ, Zhao ZW, Zhou HY, Liu YJ, Yang HJ. Systematic analysis of microRNA involved in resistance of the MCF-7 human breast cancer cell to doxorubicin. Med Oncol 2010;27:406–15.
[29] Xing B, Li WW, Sun K. A novel synthesis of high quality CdTe quantum dots with good thermal stability. Mater Lett 2008;62:3178–80.
[30] Wang Y, Zheng JW, Zhang ZJ, Yuan CW, Fu DG. CdTe nanocrystals as luminescent probes for detecting ATP, folic acid and L-cysteine in aqueous solution. Colloid Surf A 2009;342:102–6.
[31] Singh N, Manshian B, Jenkins GJ, Griffiths SM, Williams PM, Maffeis TG, et al. NanoGenotoxicology: the DNA damaging potential of engineered nanomaterials. Biomaterials 2009;30:3891–914.
[32] Prasad BR, Nikolskaya N, Connolly D, Smith TJ, Byrne SJ, Gerard VA, et al. Long-term exposure of CdTe quantum dots on PC12 cellular activity and the determination of optimum non-toxic concentrations for biological use. J Nanobiotechnology 2010;8:7.
[33] Jan E, Byrne SJ, Cuddihy M, Davies AM, Volkov Y, Gun'ko YK, et al. High-content screening as a universal tool for fingerprinting of cytotoxicity of nanoparticles. ACS Nano 2008;2:928–38.
[34] De Paoli Lacerda SH, Semberova J, Holada K, Simakova O, Hudson SD, Simak J. Carbon nanotubes activate store-operated calcium entry in human blood platelets. ACS Nano 2011;5:5808–13.
[35] Lee YS, Dutta A. MicroRNAs in cancer. Annu Rev Pathol 2009;4:199–227.
[36] Lujambio A, Calin GA, Villanueva A, Ropero S, Sanchez-Cespedes M, Blanco D, et al. A microRNA DNA methylation signature for human cancer metastasis. Proc Natl Acad Sci U S A 2008;105:13556–61.
[37] Choi AO, Brown SE, Szyf M, Maysinger D. Quantum dot-induced epigenetic and genotoxic changes in human breast cancer cells. J Mol Med 2008;86:291–302.
[38] Levine E, Ben Jacob E, Levine H. Target-specific and global effectors in gene regulation by MicroRNA. Biophys J 2007;93:L52–4.
[39] Wang X, Li Y, Xu X, Wang YH. Toward a system-level understanding of microRNA pathway via mathematical modeling. Biosystems 2010;100:31–8.
[40] Vohradsky J, Panek J, Vomastek T. Numerical modelling of microRNA-mediated mRNA decay identifies novel mechanism of microRNA controlled mRNA downregulation. Nucleic Acids Res 2010;38:4579–85.
[41] Kohler JJ, Schepartz A. Kinetic studies of Fos.Jun.DNA complex formation: DNA binding prior to dimerization. Biochemistry 2001;40:130–42.

[42] Bartlett DW, Davis ME. Insights into the kinetics of siRNA-mediated gene silencing from live-cell and live-animal bioluminescent imaging. Nucleic Acids Res 2006;34:322–33.
[43] Poliseno L, Salmena L, Zhang J, Carver B, Haveman WJ, Pandolfi PP. A coding-independent function of gene and pseudogene mRNAs regulates tumour biology. Nature 2010;465:1033–8.
[44] Kanehisa M, Goto S. KEGG: kyoto encyclopedia of genes and genomes. Nucleic Acids Res 2000;28:27–30.
[45] Walker VG, Li Z, Hulderman T, Schwegler-Berry D, Kashon ML, Simeonova PP. Potential in vitro effects of carbon nanotubes on human aortic endothelial cells. Toxicol Appl Pharmacol 2009;236:319–28.
[46] Pisanic 2nd TR, Blackwell JD, Shubayev VI, Finones RR, Jin S. Nanotoxicity of iron oxide nanoparticle internalization in growing neurons. Biomaterials 2007;28:2572–81.
[47] Auffan M, Decome L, Rose J, Orsiere T, De Meo M, Briois V, et al. In vitro interactions between DMSA-coated maghemite nanoparticles and human fibroblasts: a physicochemical and cyto-genotoxical study. Environ Sci Technol 2006;40:4367–73.
[48] Soenen SJ, Nuytten N, De Meyer SF, De Smedt SC, De Cuyper M. High intracellular iron oxide nanoparticle concentrations affect cellular cytoskeleton and focal adhesion kinase-mediated signaling. Small 2010;6:832–42.
[49] Ashburner M, Ball CA, Blake JA, Botstein D, Butler H, Cherry JM, et al. Gene ontology: tool for the unification of biology. The Gene Ontology Consortium. Nat Genet 2000;25:25–9.
[50] Lovric J, Bazzi HS, Cuie Y, Fortin GR, Winnik FM, Maysinger D. Differences in subcellular distribution and toxicity of green and red emitting CdTe quantum dots. J Mol Med 2005;83:377–85.